Application of Atomic Force Microscopy in Membrane Fouling

Subjects: Water Resources

Contributor: Mohan Wei , Yaozhong Zhang , Yifan Wang , Xiaoping Liu , Xiaoliang Li , Xing Zheng

Membrane separation technology has emerged as the preferred method for producing clean water during wastewater treatment and desalination. This preference is attributed to the high separation accuracy, energy efficiency, lack of secondary pollution, and ease of operation of the technology. Membrane fouling is a key obstacle in membrane applications, including ultrafiltration (UF), microfiltration (MF), nanofiltration (NF), and reverse osmosis (RO). Membrane fouling is a particularly serious problem in the pre-treatment processes of industrial wastewater, leading to poor water quality and increased operating costs. A thorough understanding of fouling formation and properties is required in wastewater treatment using membranes and contributes to slowing down membrane fouling and implementing appropriate control measures. In response, extensive foundational investigations of membrane fouling have been conducted, with researchers seeking to clarify primary foulants, membrane–foulant interactions, and potential fouling mitigation techniques.

membrane fouling morphology roughness interactions

1. Characterization of Membrane

The interaction between the membranes and foulants is related to the membrane surface properties, such as hydrophilicity, roughness, and charge. The development of high-quality antifouling membranes could reduce the interaction forces between foulants and membrane surfaces and decelerate membrane fouling. The technique facilitates the visualization of membrane surfaces at high resolution, characterizing three-dimensional presentation of membrane surface information, allowing for an exhaustive detailed expression of the surface characteristics of the membrane.

1.1. Characterization of Membrane Morphology

Visualization of the membrane surface morphology aids in understanding the relevant properties of the membrane. Atomic force microscopy (AFM) excels in visualizing morphological features, allowing for the in situ characterization of morphological changes occurring at the interface of functional layers on membrane surfaces during the polymerization process. During the phase inversion process, utilizing AFM to scan nanofiltration or reverse osmosis membranes prepared under various parameters in a liquid environment enables the in situ observation of more detailed and systematic changes in the surface functional layers [1]. Further, AFM can be used to investigate the degradation effects of soil microbial communities on polyethylene membranes by observing changes in the microstructure of the membrane [2]. Using AFM, it is also possible to observe the ion transport channels of

membranes. Examination of modified anion exchange membrane (AEM) materials with densely grafted ionic clusters through atomic force microscopy can reveal distinct ion conduction pathways and demonstrate that the modified AEMs exhibit excellent nano-phase separation [3]. By studying the surfaces of nanofiltration membranes using AFM in different imaging modes, various AFM imaging mode characteristics can be obtained [4]. The tapping mode in AFM allows for precise measurement of the 3D structure of soft and delicate surfaces without damaging their morphology. This technique is particularly useful for studying the interfacial polymerization process of active functional layers on nanofiltration membrane surfaces [5].

Evidently, AFM can be used to understand membrane layer surface smoothness and uniformity; capture membrane surface microscopic morphology, including surface defects, nanoscale protrusions, or depressions; and provide intuitive images of membrane surface morphology. Thus, AFM is not only capable of in situ measurement of surface morphology changes induced by hydrochemical conditions, but also enables the understanding and discovery of ion transport channels and nanoscale morphologies through 3D visualization images. Particularly, the tapping mode is almost non-destructive to thin and soft membrane surfaces. Additionally, AFM can be used to study the surface potential signals of membrane materials, overlaying them with the physicochemical properties of specific areas. These aspects are crucial for characterizing membrane performance and understanding membrane fabrication.

1.2. Characterization of Roughness

The surface roughness of a membrane is a key factor influencing interfacial performance and fouling processes. Using AFM not only allows for the observation of a membrane's surface morphology, but due to its three-dimensional measuring capabilities along the x, y, and z axes, AFM can also precisely characterize in situ the roughness of the membrane surface/functional layer and provide detailed 3D surface topography maps. AFM can be used to understand the roughness of various types of membranes, such as cation exchange membranes. During long-term operation, AFM can precisely measure changes in roughness, thereby establishing the relationship between roughness and ion exchange performance. This enhances the monitoring of the ion exchange effectiveness and contamination level of cation exchange membranes [6].

In the process of membrane modification, the incorporation of specific active components, such as surfactants or polymer monomers, in the adsorption crosslinking process can increase surface roughness and alter the structure of the membrane's functional layer. Similarly, modifications with carbon nanotubes, metal oxides, and other substances can change the membrane's morphology, increase roughness, and expand membrane channels, thereby altering the membrane's performance. Using AFM, changes in membrane surfaces and channels can be observed, and the roughness can be accurately measured. Roughness serves as an important parameter in membrane fabrication. The results generally show that the surface of the original membrane is low in roughness, uniform, and smooth. When modifiers or carbon nanotubes are added, nanoscale modified structures are formed, increasing the roughness. This enhancement in roughness can improve the membrane's anti-fouling properties, permeation evaporation performance, ion selectivity, and regulate the membrane's hydrophilicity or hydrophobicity. Asymmetric polystyrene membranes manufactured using the wet phase inversion method with the addition of

surfactant (Pluronic F127) increase the surface roughness of the membrane and strengthen the membrane channels, significantly enhancing the permeation evaporation performance of the membrane [7]. Similarly, analysis of multi-walled carbon nanotube (MWCNT) dispersed PS nanofiltration membranes [8] using AFM shows that the surface of the original PS membrane is smooth and uniform, while the addition of MWCNTs increases the surface roughness and makes the structure more evident, thus improving the hydrogen permeability of the PS membrane. Roughness measurements using AFM reveal that plasma treatment and surface acidification also increase the roughness of ion exchange membranes, enabling more ion exchange and facilitating the preparation of ion exchange membranes with excellent performance [9].

However, studies show that for rough surfaces, nanoscale modified structures have better tendencies to prevent membrane fouling, but when the modified structures are too large, they can exacerbate membrane fouling. These related insights can be obtained through the precise measurement of roughness using AFM. In addition, modifying the membrane surface through copolymerization and grafting methods can increase membrane roughness, and AFM can measure roughness changes during the membrane modification process in situ. When characterizing hydrophilic polymer-functionalized polysulfone (PSF) blend membranes using AFM [10], researchers found that the addition of 4VP side chains enhanced the surface roughness of the modified membrane. In another study, PSF membranes modified with titanium oxide compounds [11] had higher surface roughness, and these modified membranes exhibited excellent hydrophilicity and anti-fouling properties. Simple coding of the surfactants polydopamine and 3-(N, N-dimethyl myristoyl) propane sulfonate [12] can achieve anti-fouling properties of polyethersulfone (PES) ultrafiltration membranes. Scanning these modified membranes with AFM can obtain roughness parameters Rq and Ra, indicating that the modified membranes significantly mitigate flux decline and enhance anti-fouling performance.

Precise measurement of membrane surface roughness with AFM can be used to explore which roughness is more resistant to contamination on the modified membrane surface, thus achieving membrane performance adjustment. Although many studies have shown that increased roughness may lead to increased tendencies for membrane fouling [6][10], other research findings suggest that adding micrometer to nanometer-sized particles to increase surface roughness (similar to lotus leaf biomimetic structures) can reduce membrane fouling [8][9]. This discrepancy is mainly because a single roughness parameter is insufficient to summarize the complexity of membrane surface fouling. Establishing a relationship between roughness R measured with AFM and the roughness index H can more quickly and accurately evaluate membrane surface roughness [13]. In addition, an overall assessment should combine AFM with various other techniques to carefully examine membrane surface characteristics, such as surface potential, hydrophilicity/hydrophobicity, functional groups, and foulant properties. Through this comprehensive judgment of characterization results, the relationship between surface roughness and membrane fouling can be thoroughly analyzed. Establishing the relationship between membrane surface roughness measured by AFM and membrane surface potential, functional groups, etc., can better help optimize membrane hydrophilicity/hydrophobicity, permeation selectivity, ion selectivity, and anti-fouling properties, providing guidance for the design and optimization of membrane interfaces.

1.3. Measurement of Membrane Channels

Membrane channels are crucial for the filtration performance of membranes, as the size and structure of these channels directly influence the membrane's selectivity and permeation flux, which relates to the trade-off effect of the membrane. AFM has been utilized to detect various surface parameters of modified membranes, including the structure and pore size of membrane channels. These researchers [14][15][16][17][18][19] characterized the surfaces of modified membranes using AFM and found that the deposition process of modifiers made the membrane surfaces smoother, eliminating small-scale rough features, reducing pore sizes, and decreasing sensitivity to foulants. For instance, Kim et al. [15] achieved atomic-level surface functionalization of nanofiltration membranes using graphene oxide (GO) combined with plasma-enhanced atomic layer deposition (ALD) technology. A novel data analysis method [14] integrating AFM with "pore reconstruction technology" was used to assess membrane channel structures, including size, shape, and interlayer distances. The obtained membrane channel information is vital for the permeation selection process in membrane desalination and can also serve as a crucial factor in assessing the propensity for membrane fouling. AFM can precisely measure the interlayer distances of zinc oxide-coated aluminum membrane channels modified by deposition methods [16], identify the membrane channel structures of superhydrophilic copper mesh membranes coated with zinc oxide nanostructures (ZnO NW) used for oil–water separation [17], acquire information about the shape of membrane channels in modified seawater desalination nanofiltration membranes created using molecular layer deposition (MLD) techniques [18], and obtain 3D shape information of membrane channels in chitosan and polystyrene sulfonate-modified polyamide microfiltration membranes prepared by layer-by-layer (LBL) deposition methods [19].

Combining the surface and cross-sectional images obtained from AFM can construct three-dimensional images of membrane channels, providing detailed information on the size, shape, and arrangement of channels, and more accurately predicting the degree of membrane channel clogging and membrane fouling. Studies indicate that uniformly distributed pore structures, as opposed to uneven distributions, are likely to reduce the risk of fouling. The systematic distribution of pores in uniform membranes can enhance the interception capacity for foulants [20]. Notably, the geometric shape of membrane channels greatly influences membrane fouling. Typically, the fouling intensity caused by slit-shaped pores is lower than that caused by circular pores [21]. Additionally, AFM can accurately present the degree of membrane channel clogging and the state of membrane fouling in real liquid-phase environments. In contrast, SEM requires measurements under dry and vacuum conditions, which may lead to distorted results and inaccurate pore information. Therefore, membrane channel data obtained through AFM are crucial for tracking membrane fouling trajectories and assessing and improving membrane performance.

As previously mentioned, employing AFM to characterize different membranes allows for a more comprehensive observation of three-dimensional surface morphology, membrane roughness measurements, membrane channel assessments, and an overall evaluation of the material characteristics and application performance of membranes and modified membranes. As depicted in **Figure 1**, this section categorizes and summarizes the different modes, characteristics, and outcomes of modified membrane characterization via AFM as referenced in the mentioned literature. AFM has also been extensively applied in characterizing modified membranes of various materials, such as modified Langmuir–Blodgett (LB) thin films [22], uniquely shaped modified block copolymer microfiltration membranes [23], zeolite-filled polyethersulfone membranes [24], modified Carbosep M5 ceramic membranes [25], innovative positively charged nanofiltration membranes [26], organic membranes for oil–water separation [27], and

composite ceramic microfiltration membranes for greywater treatment [28]. This technique (atomic force microscopy) has become a powerful tool in the design and fabrication of functional membranes.

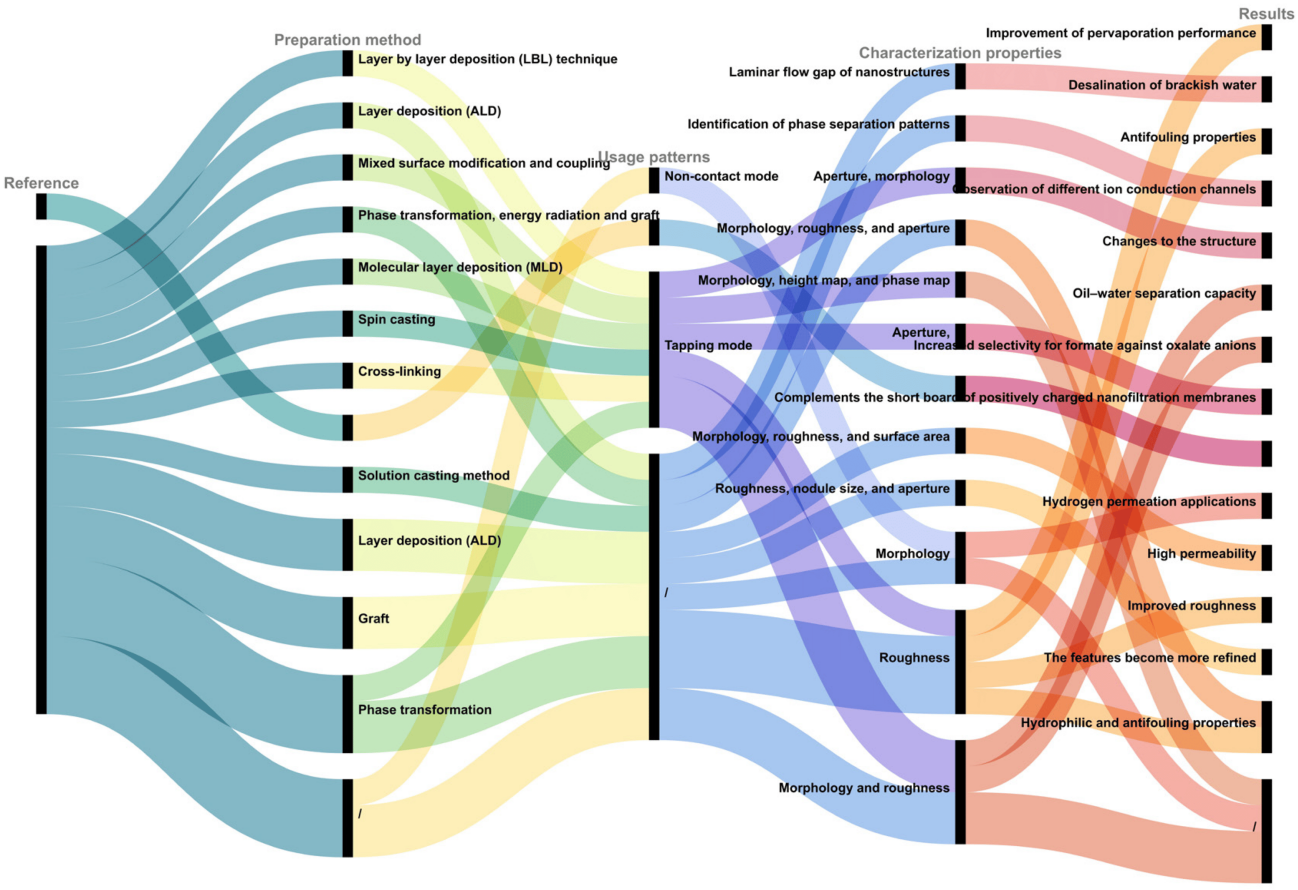

Figure 1. Different aspects and results of AFM characterization of modified membranes in different modes.

2. Characterization of Contaminants

Different types of membrane foulants are encountered in membrane-based technologies and in other techniques; therefore, employing AFM for scrutinizing the characteristics of contaminants at a microscopic level is vital. The nanometer-scale resolution of AFM enables direct observation of the contaminant morphology and structure on membrane surfaces. Accordingly, AFM could be used to monitor the adsorption and adhesion of contaminants in real-time under various environmental conditions. Morphological changes in living microorganisms during metabolism could be recorded in tapping or non-contact modes, which is a challenge for other techniques. Employing the capabilities of AFM in this way enhances understanding of membrane fouling mechanisms. Characterizing contaminants facilitates superior understanding of membrane fouling principles, and offers essential guidance for the design, operation, and maintenance of membrane filtration systems. This is an important factor in the investigation of membrane fouling mechanisms.

2.1. Organic Contaminants

Natural organic matter (NOM) is the primary contaminant in wastewater. It is a complex heterogeneous system comprising diverse organic molecules [29], such as humic substances, polysaccharides, and proteins, which can all affect the membrane performance. Observations using AFM in aquatic environments have revealed that natural polysaccharide sodium alginate (SA) predominantly exists as single helical chains, with diameters of approximately 0.2–0.3 nm [30]. Scanning humic acid sodium (HA)-contaminated mica surfaces with AFM has uncovered spherical particles and aggregates, featuring colloidal diameters under 100 nm and heights from 0.5 to 7 nm [31]. In studies on protein membrane fouling, most protein molecules have been observed as monomers on mica surfaces [32]. Extracellular organic matter (EOM) can lead to severe ultrafiltration membrane fouling. AFM enables the observation of the aggregation and blockage behaviors of pollutants on the membrane surface [33], and evaluates the effects of cleaning/pre-treatment [34]. Utilizing AFM technology aids in further understanding the impact of natural organic matter (NOM) on membrane performance during water treatment processes, thereby laying the foundation for mitigating organic membrane fouling.

2.2. Biological Contaminants

In addition to typical organic contaminants, biological contaminants can impair membrane treatment efficiency in water treatment processes. *Escherichia coli* is a common pathogenic microorganism that compromises the safety of water resources and drinking water. Researchers have used AFM to investigate the morphological changes in *E. coli* on membrane surfaces under varying pH conditions [35] and correlate it with membrane filtration and cleaning [36]. In addition, AFM has been used to examine changes in the morphology of antibiotic-resistant *E. coli* on membrane surfaces during photocatalytic Fenton water treatment [37]. Recently, owing to the potential problem of microalgae in water treatment processes, particularly in membrane treatment, AFM has been applied extensively to study microalgal cell morphology and nanomechanical properties on membrane surfaces. High-speed atomic force microscopy (HS-AFM) has been employed to analyze *Chlorella vulgaris* treated with electrocoagulation flotation (ECF) [38]. Another study used AFM to determine the energy required to disrupt individual microalgae cells [39]. Guidance could be offered for alleviating biological fouling caused by microalgae. For the living microbial cells, AFM-based single-cell force spectroscopy (AFM-SCFS) has significant value for characterizing the structure, mechanical properties, and molecular activity of individual living microbial cells [40]. The technique can measure the mechanical properties of a single microorganism, quantify individual microorganism adhesion forces, and perform structural imaging of microbial behavior while simultaneously sensing microbial activity in real-time. Wang et al. [41] employed AFM to explore the dynamic effects of various environmental factors on microorganisms and membrane surface interactions at a molecular scale. This provides a research basis for the effective inhibition of biological foulants on membrane surfaces.

AFM-SFCS allows sensitive measurements of the mechanical properties of individual molecules. This allows researchers to gain insight into the mechanical properties of individual molecules such as stretching, deformation, and fracture, which is important for understanding the properties of biomolecules, polymers, and other materials. Nevertheless, AFM-SCFS has not reached maturity yet and still presents several technical challenges. Based on the group's research on AFM-SFCS in the environmental field, researchers found that this technology faces the following problems in its application. First, the adhesion of live single cells to the probe tip is difficult and requires

the selection of suitable adhesives for cell immobilization. Additionally, assessing the viability of single cells on the probe tip after attachment is challenging, prompting researchers to explore more advanced methods for examining post-adhesion cell viability. The morphology of single cells is not consistent; it encompasses rod or spherical shapes and other irregular shapes. During the adhesion process, it is crucial to consider different adhesion positions and variations in contact areas with the measurement surface to prevent inconsistencies in the recorded force magnitudes. Furthermore, even when live cells successfully adhere, it is difficult to maintain consistent single-cell activity at the probe tip (considering the different activity levels of young and aged cells at various stages). Ongoing investigation and refinement of AFM-SCFS techniques is anticipated to address these issues in the near future. Researchers could, therefore, gain better understanding of the characteristics of biological contaminants using AFM technology, further elucidate the membrane fouling process, guide biofouling removal, and offer theoretical support and practical guidance for the development of long-lasting antifouling membrane materials and superior biofouling control strategies.

2.3. Emerging Contaminants

Emerging contaminants in wastewater treatment processes, such as microplastics, antibiotics, and endocrine-disrupting compounds (EDCs) have been attracting increasing academic attention at national and international levels. As a high-resolution tool, AFM enables a more detailed examination of the physical properties of microplastics [42]. For instance, Melo-Agustín et al. [43] employed AFM for morphological analysis of microplastic surfaces, discovering that polyethylene (PE) microplastic surfaces exhibit higher levels of roughness than polypropylene (PP) microplastic surfaces. This observation suggests that PE is more susceptible to degradation than PP, potentially leading to greater contaminant adsorption. Chen et al. [44] introduced a method that combines AFM with infrared spectroscopy (AFM-IR) to characterize nanoplastics (NPs). This hybrid AFM technique can identify and image the chemical composition of nanoplastics at a high spatial resolution (20–100 nm), thereby offering a novel approach to NP characterization. However, the large specific surface area of microplastics often causes them to function as ‘carriers’ of other contaminants during water treatment processes, which exacerbates pollution. For instance, Zhang et al. [45] employed AFM to determine the interaction forces between NPs (hematite and corundum) and *Escherichia coli* cells, gaining further understanding of the membrane fouling mechanism of microplastics.

Additionally, antibiotics are frequently occurring emerging pollutants in aquatic environments, and even at trace concentrations, antibiotics in wastewater can adversely affect human health. AFM can effectively characterize the morphology and interaction forces of antibiotics on the membrane surface, thereby enhancing the efficiency of membranes in intercepting them. For instance, Liu et al. [46] used AFM to investigate the adsorption of EDCs on nanofiltration membrane surfaces, subsequently enhancing the EDC removal rate by preparing modified nanofiltration membranes. Wu et al. [47] attached sulfamethoxazole (SMX), a representative antibiotic, to an AFM tip to measure the SMX adhesion force distribution. Their study revealed the adhesion mechanism of SMX and, potentially, that of other sulfonamide antibiotics at a molecular level from both experimental and theoretical viewpoints. Researchers have also examined the impact of microplastics on antibiotic transport during sand filtration [48] by grafting ciprofloxacin (CIP) and sulfamethoxazole (SMX) onto AFM probes to determine the

adhesion forces between representative microplastics (PS and PE) and quartz sand. Their study explored the mechanism of microplastics that enhances antibiotic transport in sand filtration systems from the perspective of molecular interactions. **Table 1** summarizes the entire literature on different aspects of AFM studies of different pollutants in this section. In summary, employing AFM to investigate contaminant morphology under various water treatment conditions contributes to a deeper understanding of the characteristics of the contaminants, which, in turn, could inform the removal of attendant membrane foulants.

Table 1. Summary of research on AFM applications in contaminants.

Research Content	AFM Model	Characterization Properties	Results	Usage Patterns	Reference
Sodium alginate (SA)	Bruker AXS Multi-mode 8, Madison, WI, USA	Morphology	Alginates exist in single coiled chains	Contact mode	[30]
Effect of Na^+ on organic fouling	Cypher ES, Oxford Instruments Asylum Research, Abingdon, UK	Morphology and interaction force	/	/	[49]
Effect of carboxyl and hydroxyl groups on adsorptive polysaccharide fouling	Cypher ES, Oxford Instruments Asylum Research, Abingdon, UK	Morphology	Transformation from 'egg box' model to formation of network gel	/	[50]
Effects of –COOH and $–NH_2$ on adsorptive polysaccharide fouling	Cypher ES, Oxford Instruments Asylum Research, Abingdon, UK	Morphology and interaction force	In pH range 4–6, adherence of polysaccharide fouling and its reversibility depend on the functional groups	Tapping mode	[51]
Effect of sodium and potassium on polysaccharide fouling on PVDF and graphene-oxide-modified PVDF membrane surfaces	Cypher ES, Oxford Instruments Asylum Research, Abingdon, UK	Interaction force	SA fouling in Na^+ condition more severe than that in K^+ owing to higher attraction forces under identical ion strengths	Tapping mode	[52]
Humic acid (HA)	Nanoscope IIIa SPM, Digital Instruments,	Morphology	Spherical particles and aggregates are found with apparent	Tapping mode	[31]

Research Content	AFM Model	Characterization Properties	Results	Usage Patterns	Reference
	Goleta, CA, USA		colloidal diameters < 100 nm and heights ranging from ~0.5 to ~7 nm		
Effect of Na^+ and Mg^{2+} on adsorptive humic acid fouling	MultiMode 8.0 AFM (Bruker, Ettlingen, Germany)	Interaction force	Cations mainly affect HA fouling by controlling electrostatic and hydration forces of membrane–HA and HA–HA	Contact mode	[53]
Effect of Ca^{2+} and Mg^{2+} on adsorptive humic acid fouling	MultiMode 8.0 AFM (Bruker, Ettlingen, Germany)	Interaction force	Mitigation mechanisms differed for both ions	/	[54]
Bovine serum albumin (BSA)	/	Morphology	Most protein molecules are spread onto mica surface as monomers	Tapping mode	[32]
Effect of chlorination and ozonation on adsorptive protein fouling	MultiMode 8.0 atomic force microscope (AFM, Bruker, Ettlingen, Germany)	Interaction force	BSA fouling definitively mitigated by pre-chlorination but enhanced by pre-ozonation	Contact mode	[53]
Flagellar morphology of *E. coli* cultured at different pH conditions	Nanowizard AFM (JPK Instrument, Berlin, Germany)	Morphology	Differences in flagellar morphology at different pH values	Contact mode	[35]
E. coli under action of different disinfectants	Digital Instruments Veeco Metrology Group, Santa Barbara, CA, USA	Morphology	Differences in cell morphology under action of different disinfectants	Tapping mode	[36]
Changes in cell morphology of antibiotic-resistant *E. coli*	Asylum Research Cypher AFM (Oxford	Morphology	Damage to *E. coli* cells eventually leads to cell lysis	/	[37]

Research Content	AFM Model	Characterization Properties	Results	Usage Patterns	Reference
	Instruments, Abingdon, UK)				
Different types of MPs	AFM diMultiMode V (Veeco, San Jose, CA, USA)	Morphology and roughness	Different types of MPs have different characteristics	/	[43]
Combined AFM and infrared spectroscopy IR (AFM-IR) characterization of MPs	/	Morphology and roughness	/	/	[44]
Forces between two NPs and *E. coli*	Agilent 5500 AFM (Molecular Imaging, Phoenix, AZ, USA)	Interaction force	Particle sizes of both hematite (α-FeO) and corundum (α-AlO) NPs significantly affected the strength of the adhesion force	Contact mode	[45]
Changes in hydrogel occurring when algae are present in the culture	HS-AFM, Bristol Nano Dynamics Ltd., Bristol, UK	Roughness	Roughness on the algal flocs significantly more pronounced than in the hydrogel layer	Contact mode	[38]
Clostridium perfringens treated by electrocoagulation floatation (ECF) method	AFM (Ntegra with Solaris platform, manufactured by NT MDT, Moscow, Russia)	Interaction force	Inefficiency of mechanical cell crushing process	Tapping mode	[39]

However, rch team embrane nts under embrane embrane with their

Ionic conditions: the research team [49][50][51][52] used AFM to study the effects of different valence ions on membrane fouling of NOMs. Using AFM force measurements, morphology characterization, and other technical methods, the effect of monovalent ions such as Na^+ and K^+ on organic compounds was found to be based on their charge and structure. However, the effect of divalent ions such as Ca^{2+} and Mg^{2+} on organic compounds also included complexation. Among them, it is closely related to the special functional groups, types, and structures of NOMs. Miao et al. [55][56] employed AFM to investigate the effects of Na^+, Mg^{2+}, and Ca^{2+} on HA fouling through HA membrane fouling experiments. These authors observed that membrane fouling intensified at lower Ca^{2+} or Mg^{2+} concentrations and significantly decreased at substantially higher Ca^{2+} or Mg^{2+} concentrations, albeit with the two ions having different mechanisms.

pH: Researchers investigated changes in membrane fouling under different pH conditions using AFM [51]. The results showed that at a pH range of 4–6, the adherence of polysaccharide fouling, and its reversibility, depended

on the functional groups. When the organics were rich in –COOH, an increase in pH reduced their deposition on the membrane surface and alleviated adsorptive fouling and irreversibility. For the $–NH_2$ functional group, an increase in pH led to more severe polysaccharide fouling owing to a lower degree of protonation, and the resulting fouling was highly irreversible. Modification using GO alleviated the adsorptive fouling of these two polysaccharides on PVDF; however, the extent of alleviation depended on the abundance of functional groups on the polysaccharides.

Time: Interestingly, researchers found that time changes could affect membrane fouling [41]. Researchers studied the pollution behavior of three selected model foulants at different adsorption times. For the SA-Ca^{2+} system, a longer adsorption time slightly increased the adsorption capacity of SA but significantly reduced its reversibility. With regards to BSA-Ca^{2+}, the extended time did not change the amount of BSA deposited on the membrane surface but led to more residual BSA after cleaning. Similarly, in the HA-Ca^{2+} system, the adsorption time had almost no effect on the adsorption amount of HA but reduced its reversibility. Duration had a significant effect on the quantity and reversibility of membrane fouling, depending on the chemical properties of the membrane. Therefore, the AFM measurement results indicate that the longer the adsorption time, the denser the fouling layer and the stronger the interaction force between the fouling membranes.

Other factors: Researchers also used AFM to study the effects of voltage on the fouling of a novel polypyrrole (PPy) and stainless steel mesh conductive composite membrane [54]. Researchers found that the PPy ‘cauliflower’ structure expanded as the applied voltage increased, and the corresponding roughness of the feature area gradually decreased from 5.91 to 4.34 nm. This result could probably be ascribed to the delocalized conjugated electron carrier in the conducting polymer moving along the polymer chain under an external electric field, which changed the dipole moment of the PPy molecules. Such change caused changes in the conformation and intermolecular arrangement of the PPy molecules, resulting in the expansion of surface morphology and, thereby, decreasing the roughness.

In addition to the these membrane fouling investigations, Arkhangelsky et al. [57] employed AFM to investigate the membrane-cleaning process and examined the influence of different cleaning agents on membrane surfaces. Analysis employing AFM revealed that the sodium hypochlorite (NaOCl) cleaning agent affected the contaminants and the membrane, leading to partial organic matter destruction and a modified membrane surface. In contrast, sodium hydroxide (NaOH) treatment completely destroyed the proteins, yielding a smooth surface with minimal residual matter. Similarly, using AFM to examine the fouling behavior of BSA on the membrane, it was found that pre-chlorination significantly mitigated membrane fouling, whereas pre-ozonation oxidation exacerbated it [53]. These studies leveraged AFM technology to characterize the morphology of common contaminants on membrane surfaces and to elucidate the alterations and characteristics of the membrane fouling surface morphology under various conditions, such as time and pH. This information provides a theoretical basis for the mechanism of converting irreversible fouling into reversible fouling, and effectively informs membrane fouling control strategies.

4. Measurement of Interactions in Membrane Fouling

In the membrane treatment process, the micro-interaction between membranes and foulants significantly affects the formation of membrane fouling. The AFM technology offers valuable insights into the characteristics of foulants and membrane–foulant interactions, which could be leveraged to develop more effective strategies for preventing and controlling membrane fouling. Such strategies include optimizing membrane materials and surface modifications, enhancing pre-treatment processes, and creating innovative cleaning and regeneration technologies, which could reduce operational costs and prolong the lifespan of the membranes. The interaction force between foulants and the membrane is crucial for determining the efficiency of membrane fouling removal. Nanomechanical measurements using AFM and the quantification of interfacial interaction forces during membrane fouling provide essential information on the nanomechanical properties of foulants and membrane surfaces. Such information is critical for understanding membrane fouling.

The type of AFM colloidal probe fabricated plays a key role for the interaction force measurements. Combining AFM with BSA-adsorbed SiO_2 microsphere colloidal probes to investigate membrane surface fouling in the presence of BSA [58]. These authors observed that the adhesion force between PVDF-BSA were −1.5 nN, whereas the adhesion force between BSA-BSA were nearly zero, suggesting that BSA fouling behavior was predominantly influenced by the physicochemical interaction between the membrane polymer and BSA. Membrane-coated colloidal probes made of SiO_2 microspheres coated with PP/PA are utilized in AFM to investigate the mechanism of membrane fouling caused by HA [59]. Force measurements showed that the interaction between the membrane and foulants was the primary factor contributing to the membrane fouling behavior. In a study of membrane fouling involving HA and SA [60], indention and retraction curves obtained from force spectroscopy measurements using an AFM probe modified with silicon nitride were used to characterize the surface stiffness and adhesive properties of fouled and clean membranes. These authors discovered that bacterial cells neither adhered to nor penetrated the organic fouling layer but, instead, traversed the thin foulant layer and directly adhered to the membrane surface.

To further understand and clarify the fouling behavior of HA and SA on membranes, Miao et al. [61] used AFM in conjunction with PVDF and foulant-coated probes to investigate the intermolecular forces between the membrane and contaminants (SA, HA, or HA/SA mixtures), as well as the forces between the contaminants themselves. Owing to the strong interaction between the hydroxyl groups in SA and PVDF, the adhesion force between PVDF and SA was more than double that of PVDF-HA. The formation of organic fouling on membranes can be studied by adsorbing the corresponding EfOM components onto the surface of PVDF microspheres sintered on cantilevers prepared to form EfOM-coated colloidal probes [62]. Using AFM, these authors demonstrated that the adhesion force between PVDF and different parts of the EfOM follow the order PVDF-TPI (affinitive) < PVDF-HPO (hydrophobic) < PVDF-HPI (hydrophilic). Several researchers have examined membrane fouling under the combined action of BSA and HA [63]. They created colloidal probes with BSA directly attached to the probe tip and employed AFM-based chemical force spectroscopy for adhesion force measurements. Furthermore, employing AFM to examine the interaction energy between polyvinyl chloride (PVC) membranes and three water contaminants, namely HA, BSA, and dextran (DEX) [64], helps in revealing the complex mechanisms of related membrane fouling.

Analyzing the AFM results for the interaction forces between individual and multiple organic contaminants with membranes has led to the following conclusions. Generally, the interaction between membranes and foulants is stronger than the interaction forces among the foulants themselves. HA adsorption significantly decreases the BSA adhesion force on hydrophobic surfaces. The fouling rate of PVC membranes follows the order of DEX > BSA > HA, demonstrating that selecting suitable pretreatment processes to remove specific foulants can effectively control polyvinyl chloride membrane fouling. Owing to the strong interaction between the hydroxyl groups in SA and PVDF, SA, rather than HA, has been identified as the primary cause of PVDF membrane fouling. This implies that the pretreatment process for removing SA is crucial in controlling PVDF membrane fouling. It suggests that employing appropriate methods, such as pretreatment, membrane modification, or cleaning, to reduce the hydrogen bonding interactions between PVDF and foulants is an effective strategy for reducing adhesion forces. Choosing pretreatments that convert HPI and HPO fractions into TPI fractions is essential for controlling PVDF membrane fouling during secondary effluent filtration. Therefore, AFM force measurements provide valuable information for selecting membrane modifications, feedwater pretreatment, and cleaning technologies in wastewater treatment and desalination.

Recently, AFM has increasingly been employed to investigate the interaction forces between various foulants and membranes. Single force spectroscopy curves from AFM are used to assess the interactions between membranes and foulants, serving as a crucial parameter for adjusting the properties of modified membranes. This technique can measure not only the interaction forces between hard objects but also those involving softer entities, such as in the interaction force measurements between pretreated modified membranes and related membrane foulants [65]. Scholars have used AFM's single force spectroscopy curves to elucidate the mechanism of scaling in electrodialysis induced by anionic polyacrylamide (APAM) in anion exchange membranes (AEM) [66]. AFM can also characterize the interaction forces between various coatings and other substances, apart from membranes, such as the interactions between bubbles in different solutions [67], dissolved organics [68], and spherical particles of asphalt coating. It can also measure the interactions between living microorganisms and membranes, which is vital since living cells, being alive, secrete exosomes under external forces and their interaction forces with membranes change under stress conditions. Using AFM to measure these forces can more accurately reflect the biological fouling on membrane surfaces. Yumiyama and others [69] directly measured the interaction forces between individual yeast cells. Scholars have also studied the adhesion forces between yeast cells and microbubbles (MB) [70]. These studies demonstrate the utility of AFM's single force spectroscopy curves in measuring the interaction forces between foulants and membranes, which can be used to evaluate the characteristics and interactions at the membrane–foulant interface. This aids in developing high-performance modified membranes and more effective membrane cleaning methods.

5. Modeling or Analysis of the Interaction in Membrane Fouling

In understanding membrane fouling processes, the characteristics of impurities (such as size, shape, charge properties, and chemical stability) and the attributes of membrane materials (such as pore size, surface roughness,

chemical stability, and charge properties) significantly influence the interaction modes between impurities and the membrane. Certain impurities could interact more strongly with specific membrane materials, potentially leading to severe membrane fouling. For example, positively charged impurities could be strongly adsorbed onto negatively charged membrane materials, forming a fouling layer. Conversely, if repulsive forces are generated between the membrane material and the impurities because of their charges, the degree of fouling could decrease. Ionic composition can also have a significant impact on foulant–foulant interactions [71]. Therefore, the modeling and analysis of such interactions could provide key insights for predicting and optimizing the performance of membrane processes.

By combining the results of AFM force measurements with certain existing theories or models, such as the extended Derjaguin–Landau–Verwey–Overbeek (XDLVO) theory [72][73] and the Hermia model [74][75], it is possible to predict the manner in which forces act as particles approach the membrane surface, as well as their impact on particle adsorption behavior. This allows for the prediction of membrane fouling based on molecular characteristics. Wang et al. [49] employed the XDLVO model to calculate the interaction energy between PVDF membranes and organic matter under different ionic strengths, finding that as the Na^+ concentration increased, the Lewis acid–base (AB) force values gradually decreased. The AB forces are related to the chemical functional groups of the particles and the membrane [76]. This result shows that an increase in ionic strength enhances the AB interaction between the membrane and organic matter, which is consistent with the total amount of organic matter adsorbed on the membrane surface as the ionic strength increases. Not only that, XDLVO interactions and surface roughness may collectively influence the transport and fate of emerging multifunctional nanohybrids in the environment [77]. In addition, these authors [78][79] found that the results calculated by the XDLVO theory aligned with the AFM analysis results, suggesting that AFM force–distance curves could effectively validate the calculated results and that AFM is highly reliable for measuring the interactions between the membrane and foulants. Integrating AFM force measurement techniques to analyze blocking mechanisms during membrane filtration [74] aids in better understanding the phenomenon of membrane fouling and in developing effective fouling prevention strategies.

The Hermia model [75], by fitting the relationship between apparent fouling resistance and membrane filtration time, identifies the types of fouling caused by different blocking mechanisms [80]. Huang et al. [81] developed the Unified Membrane Fouling Index (UMFI) based on the Hermia model. By directly testing commercial membranes, UMFI can quantify the likelihood of membrane fouling, which is very useful for evaluating fouling observed in low-pressure membranes (LPMs) across different water treatment scales. AFM force measurement technology can be used to validate these established models, helping to deepen the understanding of membrane blocking mechanisms.

It should be noted that although the XDLVO theory and Hermia model provide useful insights, they do not encompass all types of fouling behavior. These theories and models are more suitable for predictions under steady conditions, whereas actual water treatment processes are conventionally confronted by more complex, dynamic, and changing conditions. New research seeks to integrate experimental and theoretical approaches for a more comprehensive understanding and prediction of the interactions between impurities and membrane materials. For example, AFM and other nanoscale characterization techniques are used for direct observation and measurement

of the interactions between impurities and membranes, whereas molecular dynamics simulations and quantum chemical calculations are used to understand these processes at the atomic scale. Analyzing and modeling the potential interactions between different impurities and membrane materials is a key factor in membrane science and engineering. Integration of various experimental and theoretical methods is required to gain a comprehensive and in-depth understanding. In this process, AFM could predict the adsorption tendency of pollutants by measuring the interaction forces between the pollutants and the membrane surface. Further, AFM could also monitor the fouling process, such as adsorption, diffusion, and aggregation of pollutants on the membrane surface in real-time. Combining AFM with relevant theories and models helps to further the exploration of the membrane fouling process and the prediction of membrane fouling trends.

References

1. Stawikowska, J.; Livingston, A.G. Assessment of atomic force microscopy for characterisation of nanofiltration membranes. J. Membr. Sci. 2013, 425–426, 58–70.
2. Wang, P.; Song, T.; Bu, J.; Zhang, Y.; Liu, J.; Zhao, J.; Zhang, T.; Xi, J.; Xu, J.; Li, L.; et al. Does bacterial community succession within the polyethylene mulching film plastisphere drive biodegradation? Sci. Total Environ. 2022, 824, 153884.
3. He, Y.; Zhang, J.; Liang, X.; Shehzad, M.A.; Ge, X.; Zhu, Y.; Hu, M.; Yang, Z.; Wu, L.; Xu, T. Achieving high anion conductivity by densely grafting of ionic strings. J. Membr. Sci. 2018, 559, 35–41.
4. Johnson, D.J.; Al Malek, S.A.; Al-Rashdi, B.A.M.; Hilal, N. Atomic force microscopy of nanofiltration membranes: Effect of imaging mode and environment. J. Membr. Sci. 2012, 389, 486–498.
5. Olejnik, A.; Nowak, I. Atomic force microscopy analysis of synthetic membranes applied in release studies. Appl. Surf. Sci. 2015, 355, 686–697.
6. San-Martín, M.I.; Carmona, F.J.; Alonso, R.M.; Prádanos, P.; Morán, A.; Escapa, A. Assessing the ageing process of cation exchange membranes in bioelectrochemical systems. Int. J. Hydrog. Energy 2019, 44, 25287–25296.
7. Mulijani, S.; Mulanawati, A. Enhanced Performance of Asymmetric Polystyrene Membrane by Incorporation of Pluronic F127 and Its Application for Pervaporation Separation. Procedia Chem. 2012, 4, 360–366.
8. Kumar, S.; Srivastava, S.; Vijay, Y.K. Study of gas transport properties of multi-walled carbon nanotubes/polystyrene composite membranes. Int. J. Hydrog. Energy 2012, 37, 3914–3921.
9. Zafari, M.; Kikhavani, T.; Ashrafizadeh, S.N. Hybrid surface modification of an anion exchange membrane for selective separation of monovalent anions in the electrodialysis process. J.

Environ. Chem. Eng. 2022, 10, 107104.

10. Wu, C.; Zheng, J.; Hu, J. Novel antifouling polysulfone matrix membrane modified with zwitterionic polymer. J. Saudi Chem. Soc. 2021, 25, 101281.
11. Ruangdit, S.; Chittrakarn, T.; Kaew-on, C.; Samran, R.; Bootluck, W.; Sirijarukul, S. E-beam induced grafting of binary monomer on polysulfone membrane for the separation of skim natural rubber latex. J. Environ. Chem. Eng. 2022, 10, 107862.
12. Nie, Z.; Liu, C.; Jiang, X.; Zhou, Y.; Lin, X.; Zhao, X.; He, Q.; Chai, H.; Pang, X.; Ma, J. Dopamine-triggered one-step codeposition of zwitterionic surfactants for anti-fouling polyethersulfone ultrafiltration membrane modification. Appl. Surf. Sci. 2022, 598, 153871.
13. Johnson, D.; Hilal, N. Polymer membranes—Fractal characteristics and determination of roughness scaling exponents. J. Membr. Sci. 2019, 570–571, 9–22.
14. ElHadidy, A.M.; Peldszus, S.; Van Dyke, M.I. Development of a pore construction data analysis technique for investigating pore size distribution of ultrafiltration membranes by atomic force microscopy. J. Membr. Sci. 2013, 429, 373–383.
15. Kim, T.N.; Lee, J.; Choi, J.H.; Ahn, J.H.; Yang, E.; Hwang, M.H.; Chae, K.J. Tunable atomic level surface functionalization of a multi-layered graphene oxide membrane to break the permeability-selectivity trade-off in salt removal of brackish water. Sep. Purif. Technol. 2021, 274, 119047.
16. Mahmodi, G.; Ronte, A.; Dangwal, S.; Wagle, P.; Echeverria, E.; Sengupta, B.; Vatanpour, V.; McLlroy, D.N.; Ramsey, J.D.; Kim, S.-J. Improving antifouling property of alumina microfiltration membranes by using atomic layer deposition technique for produced water treatment. Desalination 2022, 523, 115400.
17. Huang, A.; Kan, C.-C.; Lo, S.-C.; Chen, L.-H.; Su, D.-Y.; Soesanto, J.F.; Hsu, C.-C.; Tsai, F.-Y.; Tung, K.-L. Nanoarchitectured design of porous ZnO@copper membranes enabled by atomic-layer-deposition for oil/water separation. J. Membr. Sci. 2019, 582, 120–131.
18. Welch, B.C.; McIntee, O.M.; Myers, T.J.; Greenberg, A.R.; Bright, V.M.; George, S.M. Molecular layer deposition for the fabrication of desalination membranes with tunable metrics. Desalination 2021, 520, 115334.
19. Chandra, P.N.; Usha, K.; Mohan, M.K. Design, development and characterization of polyelectrolyte multilayer membranes for potential filtration applications. Mater. Today Proc. 2021, 41, 530–534.
20. Zhang, N.; Yang, X.; Wang, Y.; Qi, Y.; Zhang, Y.; Luo, J.; Cui, P.; Jiang, W. A review on oil/water emulsion separation membrane material. J. Environ. Chem. Eng. 2022, 10, 107257.
21. Ullah, A.; Tanudjaja, H.J.; Ouda, M.; Hasan, S.W.; Chew, J.W. Membrane fouling mitigation techniques for oily wastewater: A short review. J. Water Process Eng. 2021, 43, 102293.

22. Meral, K.; Erbil, H.Y.; Onganer, Y. A spectroscopic study of water-soluble pyronin B and pyronin Y in Langmuir–Blodgett films mixed with stearic acid. Appl. Surf. Sci. 2011, 258, 1605–1612.
23. Allen, F.I.; Ercius, P.; Modestino, M.A.; Segalman, R.A.; Balsara, N.P.; Minor, A.M. Deciphering the three-dimensional morphology of free-standing block copolymer thin films by transmission electron microscopy. Micron 2013, 44, 442–450.
24. Chakraborty, S.; Wang, B.; Dutta, P.K. Tolerance of polymer-zeolite composite membranes to mechanical strain. J. Membr. Sci. 2016, 518, 192–202.
25. Llanos, J.; Williams, P.M.; Cheng, S.; Rogers, D.; Wright, C.; Perez, A.; Canizares, P. Characterization of a ceramic ultrafiltration membrane in different operational states after its use in a heavy-metal ion removal process. Water Res. 2010, 44, 3522–3530.
26. Cheng, S.; Oatley, D.L.; Williams, P.M.; Wright, C.J. Positively charged nanofiltration membranes: Review of current fabrication methods and introduction of a novel approach. Adv. Colloid Interface Sci. 2011, 164, 12–20.
27. Ni, T.; You, Y.; Xie, Z.; Kong, L.; Newman, B.; Henderson, L.; Zhao, S. Waste-derived carbon fiber membrane with hierarchical structures for enhanced oil-in-water emulsion separation: Performance and mechanisms. J. Membr. Sci. 2022, 653, 120543.
28. Jafari, B.; Rezaei, E.; Dianat, M.J.; Abbasi, M.; Hashemifard, S.A.; Khosravi, A.; Sillanpää, M. Development of a new composite ceramic membrane from mullite, silicon carbide and activated carbon for treating greywater. Ceram. Int. 2021, 47, 34667–34675.
29. Teng, J.; Wu, M.; Chen, J.; Lin, H.; He, Y. Different fouling propensities of loosely and tightly bound extracellular polymeric substances (EPSs) and the related fouling mechanisms in a membrane bioreactor. Chemosphere 2020, 255, 126953.
30. Hu, C.; Lu, W.; Sun, C.; Zhao, Y.; Zhang, Y.; Fang, Y. Gelation behavior and mechanism of alginate with calcium: Dependence on monovalent counterions. Carbohydr. Polym. 2022, 294, 119788.
31. Chen, C.; Wang, X.; Jiang, H.; Hu, W. Direct observation of macromolecular structures of humic acid by AFM and SEM. Colloids Surf. A Physicochem. Eng. Asp. 2007, 302, 121–125.
32. Demaneche, S.; Chapel, J.P.; Monrozier, L.J.; Quiquampoix, H. Dissimilar pH-dependent adsorption features of bovine serum albumin and alpha-chymotrypsin on mica probed by AFM. Colloids Surf. B Biointerfaces 2009, 70, 226–231.
33. Gao, K.; Li, T.; Zhao, Q.; Liu, W.; Liu, J.; Song, Y.; Chu, H.; Dong, B. UF fouling behavior of allelopathy of extracellular organic matter produced by mixed algae co-cultures. Sep. Purif. Technol. 2021, 261, 118297.

34. Song, W. Nanofiltration of natural organic matter with H2O2/UV pretreatment: Fouling mitigation and membrane surface characterization. J. Membr. Sci. 2004, 241, 143–160.
35. Chang, K.C.; Cheng, S.J.; Chen, Y.C.; Huang, H.R.; Liou, J.W. Nanoscopic analysis on pH induced morphological changes of flagella in Escherichia coli. J. Microbiol. Immunol. Infect. 2013, 46, 405–412.
36. Zorila, F.L.; Ionescu, C.; Craciun, L.S.; Zorila, B. Atomic force microscopy study of morphological modifications induced by different decontamination treatments on Escherichia coli. Ultramicroscopy 2017, 182, 226–232.
37. Ahmed, Y.; Zhong, J.; Yuan, Z.; Guo, J. Simultaneous removal of antibiotic resistant bacteria, antibiotic resistance genes, and micropollutants by a modified photo-Fenton process. Water Res. 2021, 197, 117075.
38. Landels, A.; Beacham, T.A.; Evans, C.T.; Carnovale, G.; Raikova, S.; Cole, I.S.; Goddard, P.; Chuck, C.; Allen, M.J. Improving electrocoagulation floatation for harvesting microalgae. Algal Res. 2019, 39, 101446.
39. Lee, A.K.; Lewis, D.M.; Ashman, P.J. Force and energy requirement for microalgal cell disruption: An atomic force microscope evaluation. Bioresour. Technol. 2013, 128, 199–206.
40. Li, M. Chapter 7—Nanoscale imaging and force probing of single microbial cells by atomic force microscopy. In Atomic Force Microscopy for Nanoscale Biophysics; Li, M., Ed.; Academic Press: Cambridge, MA, USA, 2023; pp. 187–217.
41. Wang, Y.; Zheng, X.; Xiao, K.; Xue, J.; Ulbricht, M.; Zhang, Y. How and why does time matter—A comparison of fouling caused by organic substances on membranes over adsorption durations. Sci. Total Environ. 2023, 866, 160655.
42. Cai, L.; Wu, D.; Xia, J.; Shi, H.; Kim, H. Influence of physicochemical surface properties on the adhesion of bacteria onto four types of plastics. Sci. Total Environ. 2019, 671, 1101–1107.
43. Melo-Agustin, P.; Kozak, E.R.; de Jesus Perea-Flores, M.; Mendoza-Perez, J.A. Identification of microplastics and associated contaminants using ultra high resolution microscopic and spectroscopic techniques. Sci. Total Environ. 2022, 828, 154434.
44. Chen, Y.; Wen, D.; Pei, J.; Fei, Y.; Ouyang, D.; Zhang, H.; Luo, Y. Identification and quantification of microplastics using Fourier-transform infrared spectroscopy: Current status and future prospects. Curr. Opin. Environ. Sci. Health 2020, 18, 14–19.
45. Zhang, W.; Stack, A.G.; Chen, Y. Interaction force measurement between E. coli cells and nanoparticles immobilized surfaces by using AFM. Colloids Surf. B Biointerfaces 2011, 82, 316–324.

46. Liu, Y.; Yuan, S.; Chi, M.; Wang, Y.; Van Eygen, G.; Zhao, R.; Zhang, X.; Li, G.; Volodine, A.; Hu, S.; et al. Efficient capture of endocrine-disrupting compounds by a high-performance nanofiltration membrane for wastewater treatment. Water Res. 2022, 227, 119322.
47. Wu, J.; Lu, L.; Wang, R.; Pan, L.; Chen, B.; Zhu, X. Influence of microplastics on the transport of antibiotics in sand filtration investigated by AFM force spectroscopy. Sci. Total Environ. 2023, 873, 162344.
48. Wu, J.; Wang, R.; Zhang, Y.; Chen, B.; Zhu, X. In situ scrutinize the adsorption of sulfamethoxazole in water using AFM force spectroscopy: Molecular adhesion force determination and fractionation. J. Hazard. Mater. 2022, 426, 128128.
49. Zhai, Y.; Bai, D.; Wang, Y.; Zhang, Y.; Qi, Y.; Qiu, X.; Wang, Y.-f.; Wang, Y.X.; Zheng, X. Effect of Na+ on organic fouling depends on Na+ concentration and the property of the foulants. Desalination 2022, 531, 115709.
50. Zhang, Y.; Wang, Y.; Cao, X.; Xue, J.; Zhang, Q.; Tian, J.; Li, X.; Qiu, X.; Pan, B.; Gu, A.Z.; et al. Effect of carboxyl and hydroxyl groups on adsorptive polysaccharide fouling: A comparative study based on PVDF and graphene oxide (GO) modified PVDF surfaces. J. Membr. Sci. 2020, 595, 117514.
51. Wang, Y.; Zheng, X.; Wang, Z.; Shi, Z.; Kong, Z.; Zhong, M.; Xue, J.; Zhang, Y. Effects of –COOH and –NH2 on adsorptive polysaccharide fouling under varying pH conditions: Contributing factors and underlying mechanisms. J. Membr. Sci. 2021, 621, 118933.
52. Wang, Y.; Zheng, X.; Li, D.; Meng, F.; Tian, J.; Wang, M.; Li, L.; Wu, H.; Zhang, Y. Effect of sodium and potassium on polysaccharide fouling on PVDF and graphene oxide modified PVDF membrane surfaces. Process Saf. Environ. Prot. 2022, 165, 387–395.
53. Miao, R.; Zhou, Y.; Wang, P.; Lu, W.; Li, P.; Li, X.; Wang, L. A comparison of effect mechanisms of chlorination and ozonation on the interfacial forces of protein at membrane surfaces and the implications for membrane fouling control. J. Membr. Sci. 2021, 628, 119266.
54. Zhang, Y.; Wang, T.; Meng, J.; Lei, J.; Zheng, X.; Wang, Y.; Zhang, J.; Cao, X.; Li, X.; Qiu, X.; et al. A novel conductive composite membrane with polypyrrole (PPy) and stainless-steel mesh: Fabrication, performance, and anti-fouling mechanism. J. Membr. Sci. 2020, 621, 118937.
55. Miao, R.; Wang, L.; Deng, D.; Li, S.; Wang, J.; Liu, T.; Zhu, M.; Lv, Y. Evaluating the effects of sodium and magnesium on the interaction processes of humic acid and ultrafiltration membrane surfaces. J. Membr. Sci. 2017, 526, 131–137.
56. Miao, R.; Li, X.; Wu, Y.; Wang, P.; Wang, L.; Wu, G.; Wang, J.; Lv, Y.; Liu, T. A comparison of the roles of Ca2+ and Mg2+ on membrane fouling with humic acid: Are there any differences or similarities? J. Membr. Sci. 2018, 545, 81–87.

57. Arkhangelsky, E.; Bazarbayeva, A.; Kamal, A.; Kim, J.; Inglezakis, V.; Gitis, V. Tangential streaming potential, transmembrane flux, and chemical cleaning of ultrafiltration membranes. Sep. Purif. Technol. 2021, 258, 118045.

58. Hashino, M.; Hirami, K.; Ishigami, T.; Ohmukai, Y.; Maruyama, T.; Kubota, N.; Matsuyama, H. Effect of kinds of membrane materials on membrane fouling with BSA. J. Membr. Sci. 2011, 384, 157–165.

59. Meng, X.R.; Tang, W.T.; Wang, L.; Wang, X.D.; Huang, D.X.; Chen, H.N.; Zhang, N. Mechanism analysis of membrane fouling behavior by humic acid using atomic force microscopy: Effect of solution pH and hydrophilicity of PVDF ultrafiltration membrane interface. J. Membr. Sci. 2015, 487, 180–188.

60. Heffernan, R.; Habimana, O.; Semiao, A.J.; Cao, H.; Safari, A.; Casey, E. A physical impact of organic fouling layers on bacterial adhesion during nanofiltration. Water Res. 2014, 67, 118–128.

61. Gao, Z.; Mi, N.; Liu, T. Preparation of a polyvinylidene fluoride membrane material probe and its application in membrane fouling research. Desalination 2015, 357, 171–177.

62. Miao, R.; Wang, L.; Lv, Y.; Wang, X.; Feng, L.; Liu, Z.; Huang, D.; Yang, Y. Identifying polyvinylidene fluoride ultrafiltration membrane fouling behavior of different effluent organic matter fractions using colloidal probes. Water Res. 2014, 55, 313–322.

63. Wang, Y.; Zheng, X.; Li, D.; Tian, J.; Wu, H.; Zhang, Y. Comparison of membrane fouling induced by protein, polysaccharide and humic acid under sodium and calcium ionic conditions. Desalination 2023, 548, 116236.

64. Fu, W.; Wang, L.; Chen, F.; Zhang, X.; Zhang, W. Polyvinyl chloride (PVC) ultrafiltration membrane fouling and defouling behavior: EDLVO theory and interface adhesion force analysis. J. Membr. Sci. 2018, 564, 204–210.

65. Mozia, S.; Darowna, D.; Orecki, A.; Wróbel, R.; Wilpiszewska, K.; Morawski, A.W. Microscopic studies on TiO2 fouling of MF/UF polyethersulfone membranes in a photocatalytic membrane reactor. J. Membr. Sci. 2014, 470, 356–368.

66. Guo, H.; Xiao, L.; Yu, S.; Yang, H.; Hu, J.; Liu, G.; Tang, Y. Analysis of anion exchange membrane fouling mechanism caused by anion polyacrylamide in electrodialysis. Desalination 2014, 346, 46–53.

67. Englert, A.H.; Ren, S.; Masliyah, J.H.; Xu, Z. Interaction forces between a deformable air bubble and a spherical particle of tuneable hydrophobicity and surface charge in aqueous solutions. J. Colloid Interface Sci. 2012, 379, 121–129.

68. Zhang, S.; Gutierrez, L.; Niu, X.Z.; Qi, F.; Croue, J.P. The characteristics of organic matter influence its interfacial interactions with MnO(2) and catalytic oxidation processes. Chemosphere 2018, 209, 950–959.

69. Villacorte, L.O.; Ekowati, Y.; Neu, T.R.; Kleijn, J.M.; Winters, H.; Amy, G.; Schippers, J.C.; Kennedy, M.D. Characterisation of algal organic matter produced by bloom-forming marine and freshwater algae. Water Res. 2015, 73, 216–230.
70. Yumiyama, S.; Kato, S.; Konishi, Y.; Nomura, T. Direct measurement of interaction forces between a yeast cell and a microbubble using atomic force microscopy. Colloids Surf. A Physicochem. Eng. Asp. 2019, 583, 123963.
71. Wu, J.; Contreras, A.E.; Li, Q. Studying the impact of RO membrane surface functional groups on alginate fouling in seawater desalination. J. Membr. Sci. 2014, 458, 120–127.
72. Tang, C.Y.; Chong, T.H.; Fane, A.G. Colloidal interactions and fouling of NF and RO membranes: A review. Adv. Colloid Interface Sci. 2011, 164, 126–143.
73. Brant, J.A.; Childress, A.E. Assessing short-range membrane–colloid interactions using surface energetics. J. Membr. Sci. 2002, 203, 257–273.
74. Zhenga, Y.; Zhanga, W.; Tanga, B.; Bina, L.; Dinga, J. Membrane fouling mechanism of biofilm-membrane bioreactor (BF-MBR): Pore blocking model and membrane cleaning. Bioresour. Technol. 2018, 250, 398.
75. Gomes, M.C.S.; Moreira, W.M.; Paschoal, S.M.; Sipoli, C.C.; Suzuki, R.M.; Sgorlon, J.G.; Pereira, N.C. Modeling Of Fouling Mechanisms In The Biodiesel Purification Using Ceramic Membranes. Sep. Purif. Technol. 2021, 269, 118595.
76. Lin, T.; Lu, Z.J.; Chen, W. Interaction mechanisms and predictions on membrane fouling in an ultrafiltration system, using the XDLVO approach. J. Membr. Sci. 2014, 461, 49–58.
77. Xia, T.; Li, S.; Wang, H.; Guo, C.; Liu, C.; Liu, A.; Guo, X.; Zhu, L. Insights into the Transport of Pristine and Photoaged Graphene Oxide-Hematite Nanohybrids in Saturated Porous Media: Impacts of XDLVO Interactions and Surface Roughness. J. Hazard. Mater. 2021, 419, 126488.
78. Li, R.; Lou, Y.; Xu, Y.; Ma, G.; Liao, B.Q.; Shen, L.; Lin, H. Effects of surface morphology on alginate adhesion: Molecular insights into membrane fouling based on XDLVO and DFT analysis. Chemosphere 2019, 233, 373–380.
79. Ou, Q.; Xu, Y.; Li, X.; He, Q.; Liu, C.; Zhou, X.; Wu, Z.; Huang, R.; Song, J.; Huangfu, X. Interactions between activated sludge extracellular polymeric substances and model carrier surfaces in WWTPs: A combination of QCM-D, AFM and XDLVO prediction. Chemosphere 2020, 253, 126720.
80. Shee Keat, M. Membrane Technology for Glycerin Purification. Doctoral Dissertation, Monash University, Faculty of Engineering, Chemical Engineering, Clayton, Malaysia, 2017. Available online: https://bridges.monash.edu/articles/thesis/Membrane_technology_for_glycerin_purification/4652773 (accessed on 1 May 2023).

81. Huang, H.; Young, T.A.; Jacangelo, J.G. Unified Membrane Fouling Index for Low Pressure Membrane Filtration of Natural Waters: Principles and Methodology. Environ. Sci. Technol. 2008, 42, 714.